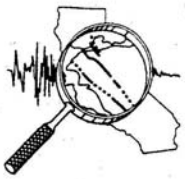

Johnston, M.J.S., Myren, G.D., Mueller, R.J., Linde, A.T., and Gladwin, M.T., 1992, A focused earthquake prediction experiment on the southern Hayward fault: Detection array and expected strains and displacements during fault rupture, *in* Borchardt, Glenn, and others, eds., Proceedings of the Second Conference on Earthquake Hazards in the Eastern San Francisco Bay Area: California Department of Conservation, Division of Mines and Geology Special Publication 113, p.197-206.

A Focused Earthquake Prediction Experiment on the Southern Hayward Fault: Detection Array and Expected Strains and Displacements During Fault Rupture

By
Malcolm J. S. Johnston[1], G. Douglas Myren[1], Robert J. Mueller[1],
Alan T. Linde[2], and Michael T. Gladwin[3]

ABSTRACT

The identification of reliable short- and intermediate-term precursors to damaging earthquakes remains a critical challenge to the earthquake hazard reduction program. To this end, we are installing a focused earthquake monitoring experiment on the southern segment of the Hayward fault. Instruments to be used in this experiment include, dilational strainmeters, tensor strainmeters, water well monitors, creepmeters, continuous GPS displacement monitors, seismic velocity and acceleration transducers. The borehole array of eight to ten sites, is located between San Leandro and Milpitas with most sites at distances from 2 km to 7 km from the Hayward Fault. Data are transmitted to Menlo Park via digital satellite telemetry. The instrument package (strainmeter, seismometer and acclerometer) at each site is installed at a depth of about 200 m where the measurement precision is about 20 dB below that of near-surface installations and short-term changes in strain of less than one part per billion (ppb) can be identified. Continuous GPS displacement monitors are installed near the north end of the array. Surface fault displacement is being monitored initially with three creepmeters installed in the City of Hayward. The overall array design was influenced by the form and amplitude of strain and displacement fields calculated from simple dislocation models of possible damaging earthquakes that might occur on either the southern segment of the Hayward fault, or on the Calaveras fault.

INTRODUCTION

The U.S. Geological Survey, in cooperation with several scientific institutions, is installing a variety of seismic and deformation monitoring instruments at selected sites along the southern segment of the Hayward Fault (Figure 1). The coordinated instrument array is installed in deep boreholes a few kilometers from the fault to capture the initiation of fault failure at depths where earthquakes occur. We measure ground strain, heat flow water level, seismic velocity, seismic acceleration, and underground temperature. Instruments installed at depths between 150-m and 300-m send continuous data to monitoring computers at the USGS West Region Headquarters in Menlo Park.

The magnitude of expected earthquakes in this region is an important issue. The "size" of an earthquake can best be described by a parameter called the seismic moment. Seismic moment, M, is given (Aki, 1987) by:

$$M = \mu SLW$$

where μ is the shear modulus, S is the amount of slip, L is the rupture length, and W is the rupture width. The seismic moment is related to the local magnitude M_L by;

$$M_L = 0.66 \log M + 10.6$$

If the Hayward fault ruptured between San Leandro and southeastern Fremont L=30 km), to a depth of 10 kilometers (W=10 km), with 1 meter of slip (S=1 m), this would produce an earthquake between *M* 6.5 and 7. The distribution of earth-

[1]U. S. Geological Survey, 345 Middlefield Road, MS977, Menlo Park, CA 94025
[2]Carnegie Institution of Washington, Washington, DC 20015
[3]Physics Department, University of Queensland, Australia 4067

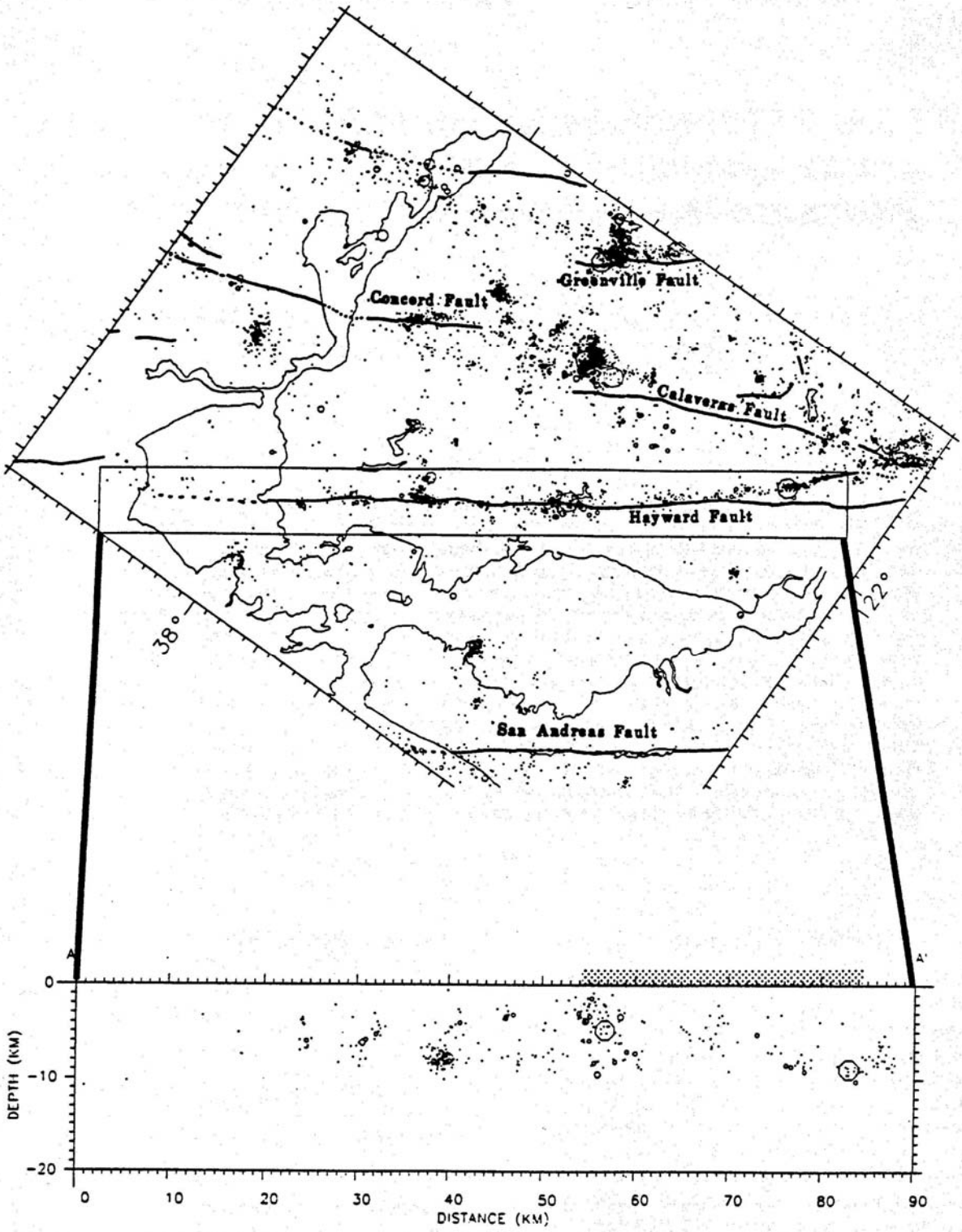

Figure 1. Earthquakes located in the San Francisco Bay area between 1969 and 1989 shown in map view in the upper plot and in crossection in the lower plot. The hatched area in the bottom plot shows the 30-km long region chosen for intensive study.

quakes on the fault plane (Figure 1, lower plot) suggests that such an earthquake would fill the apparent gap in seismicity in this region (Figures 1 and 2). An altemate scenario might involve a series of magnitude 5 to 6 earthquakes, with more than 30 magnitude 5.5 earthquakes being required to produce the same moment release as one magnitude 6.5 earthquake.

Large earthquakes should be preceded by changes in crustal stress and strain in the epicentral region (Mogi, 1985). Although some intriguing indications of impending fault failure have been reported (Rikitake, 1976; Mogi, 1985; Kanamori and Cipar, 1974; Linde and others, 1988), these signals are not routinely observed. Instrument sensitivity has increased and the effects of near-surface earth noise have been dramatically reduced (Sacks and others, 1971; Wyatt and others, 1982), but quantification of "precursive" strain and tilt changes and identification of the underlying physics of failure have proven illusive (Johnston and others, 1987). Arrays of borehole instruments have been installed in Japan [see summary of the Japanese Program in Mogi (1981a)] and at several critical locations within the San Andreas fault system (Johnston and others, 1987) to clarify this issue. The southem Hayward fault has been chosen as another of these critical locations.

We have already completed the initial drilling, installation of downhole seismometers, and part installation of the downhole strainmeters. We have measured heat flow, determined borehole lithology, and obtained samples of the core. In this paper, we discuss the likely sequence of events that could lead to failure of the Hayward fault. We have calculated the expected displacements and strains at points around the Hayward fault for events with magnitudes 4, 5, 6, and 6.5.

INSTRUMENTATION

In expectation of a moderate to large magnitude earthquake in the East Bay, possibly on the southem segment of the Hayward fault or on the Calaveras fault, seven deep borehole dilational strainmeters, six 3-component borehole seismometers, two tensor strainmeters, several creepmeters and monitored water wells are being installed along the southem Hayward fault in 1992 (Figure 2). Also shown on Figure 2 (open squares) are the locations of earthquakes with magnitude greater than 4 that have occurred in this region since 1969.

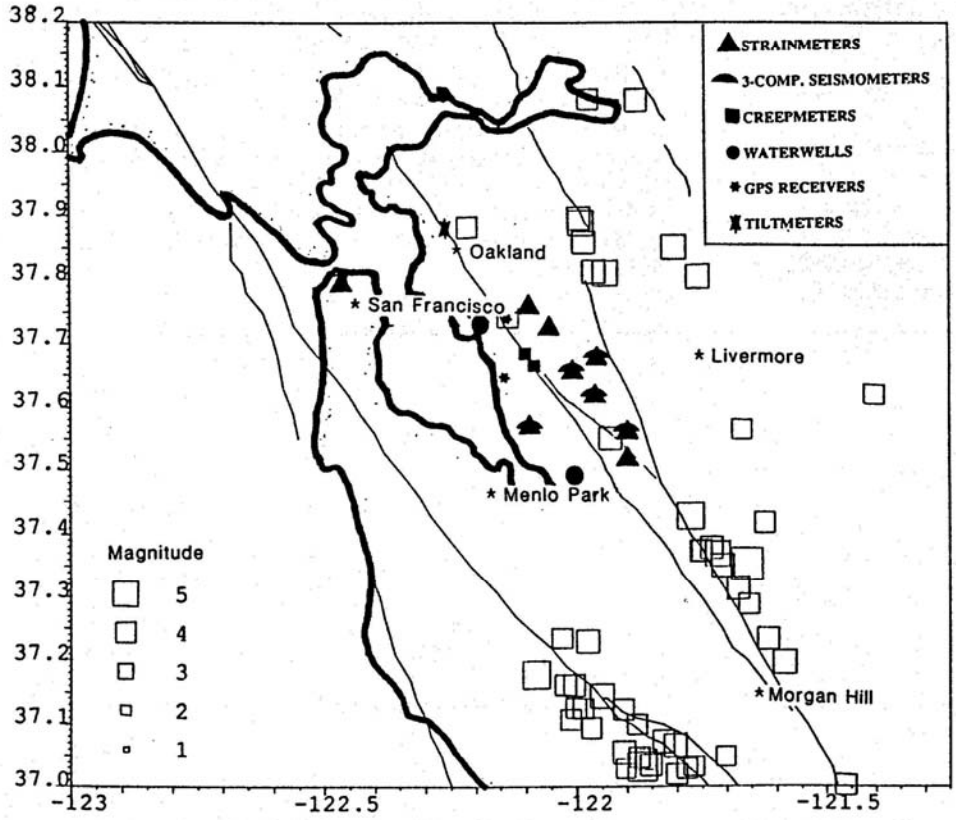

Figure 2. Location of proposed borehole strainmeter (triangles), borehole seismometers, water well (circles), and continuous fault creep monitoring sites (squares) along the Hayward Fault. Sites with three-component borehole seismometers already installed are shown as open circles within the borehole triangles.

Strainmeters are instruments designed to detect minute ground deformation (to better than one part per billion) by measuring relative expansion or contraction of the strainmeter anchor points. While the dilational strainmeters measure change in volumetric strain (Sacks and others, 1971), the tensor strainmeters monitor strain in three independent directions (Gladwin, 1984). To avoid cultural and other noise at the earth's surface, both types of straimeters are permanently cemented in the bottom of boreholes with special expansive grout.

Creepmeters continuously measure fault movement or slippage that occurs aseismically - sometimes smoothly and sometimes in episodes. The instrument consists of a buried wire, 10 to 30 m long, anchored at one end but free to move through monitoring devices at the other (Schultz and Burford, 1979). Three creepmeters are currently installed across the Hayward fault in downtown Hayward.

Changes in ground strain either squeeze or stretch underground water reservoirs and cause the water level in wells to rise or fall much like water in the neck of a water-filled balloon. By precisely monitoring the water level with pressure transducers, indications of dilational strain changes in the surrounding region can be detected.

The dilational and tensor strainmeters used in this study will be installed at depths of about 200-m below the surface (Figure 2) and operate at sensitivities of better than 10^{-10} and 10^{-9}, respectively. The sensors are cemented in boreholes with expansive grout and each borehole is then filled to the surface with cement to avoid long-term strain changes due to hole relaxation effects and re-equilibration of the aquifer system.

The strain, creep and water level data are transmitted with 16-bit and 12-bit digital telemetry through the GOES satellite to Menlo Park at 1 sample every 10 minutes (Silverman and others, 1989). Strain and seismic data will be recorded on site with 16-bit digital recorders (Borcherdt and others, 1985). The strain sensors, the site, and the telemetry system are calibrated with solid earth tides corrected for ocean-load. This calibration is repeatable to better than 5% and has remained stable through earthquakes to better than 1%.

NON-LINEAR STRAIN PRECEDING FAILURE

Both theoretical models (Kostrov, 1966; Richards, 1976; Andrews, 1976; Freund, 1979; Rice and Rudnicki, 1979; Rice, 1983; Stuart, 1979; Stuart and Mavko, 1979; Das and Scholz, 1981; Rundle and others, 1984) and laboratory observations of fault failure (Dieterich, 1979; Mogi, 1981b; Mogi and others, 1982) indicate that non-linear strain precedes rupture. Thus, detection of these strain changes should lead to a method for predicting the dynamic slip instability that results in an earthquake.

It is not clear from these model studies and laboratory measurements whether the entire rupture zone exhibits non-linear behavior (as implied by "preparation zone" terminology (Sadovsky and others, 1972)) or whether a small region of higher strength fails and, by drawing on the elastic strain energy in the region, triggers rupture over the entire zone. In the first case, arrays of sensitive strain and tilt instruments should readily detect accelerating deformation. The expected signals have an easily identifiable form (nonlinear exponential strain increase) during the period immediately preceding rupture initiation. Also, the total slip moment (preseismic, coseismic and post-seismic) can be determined when each phase of the rupture process is identified. In the second case, failure initiates in small regions of high strength and expands to arbitrary size until stopped by mechanical or geometrically strong barriers. Here, detection of preseismic slip and, more importantly, prediction of the final rupture size is difficult (Brune, 1979). Unfortunately, the best evidence obtained during the past 10 years indicates that the latter possibility occurs in strike slip regimes in California and in thrust regimes in Japan (Johnston and others, 1987)

This issue is further complicated where faults are weak as a result of high fluid pressures. This results either from low permeability fault zone materials (Byerlee and others, 1990) or from dynamic injection of fluid from below into the fault (Rice, 1992). For any of these cases, the form of the signal expected during the final stages of failure should be that shown in the Figure 3. The amplitude of this signal at a particular strainmeter, ground displacement monitor (GPS) or water well monitor will, of course, depend on the area of fault that is failing, the amount of nonlinear strain that is occurring, and the relative location of the instrument with respect to the failing region.

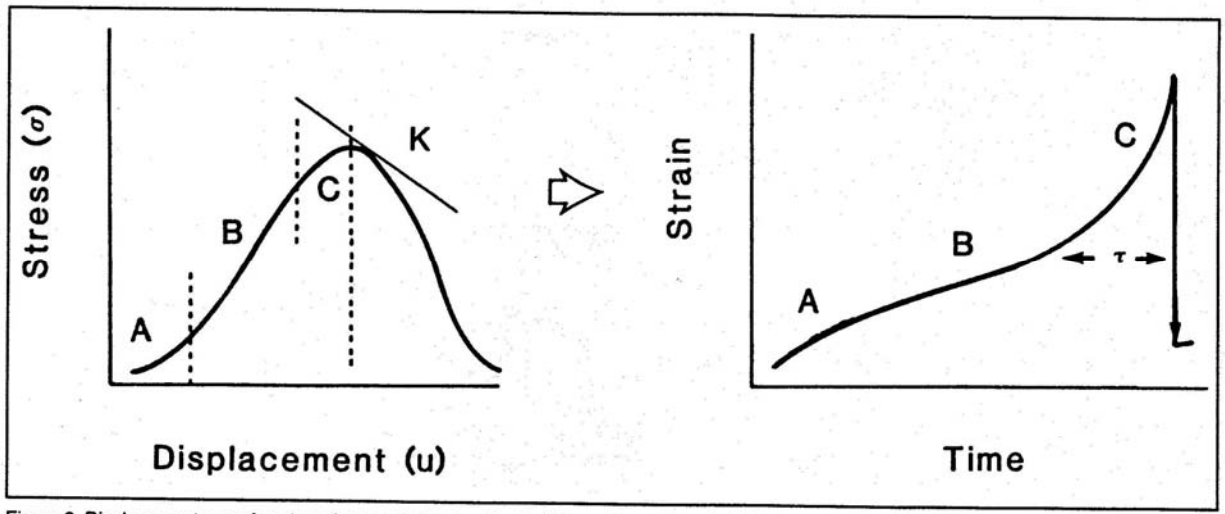

Figure 3. Displacement as a function of stress during loading to failure of crustal rocks (left side). Strain within these rocks as a function of time during this process (see Stuart, 1979). The parts of the curve A, B, and C represent primary, secondary, and tertiary creep in the rock as failure is approached. ~ represents the period after which non-linear strain is first detected.

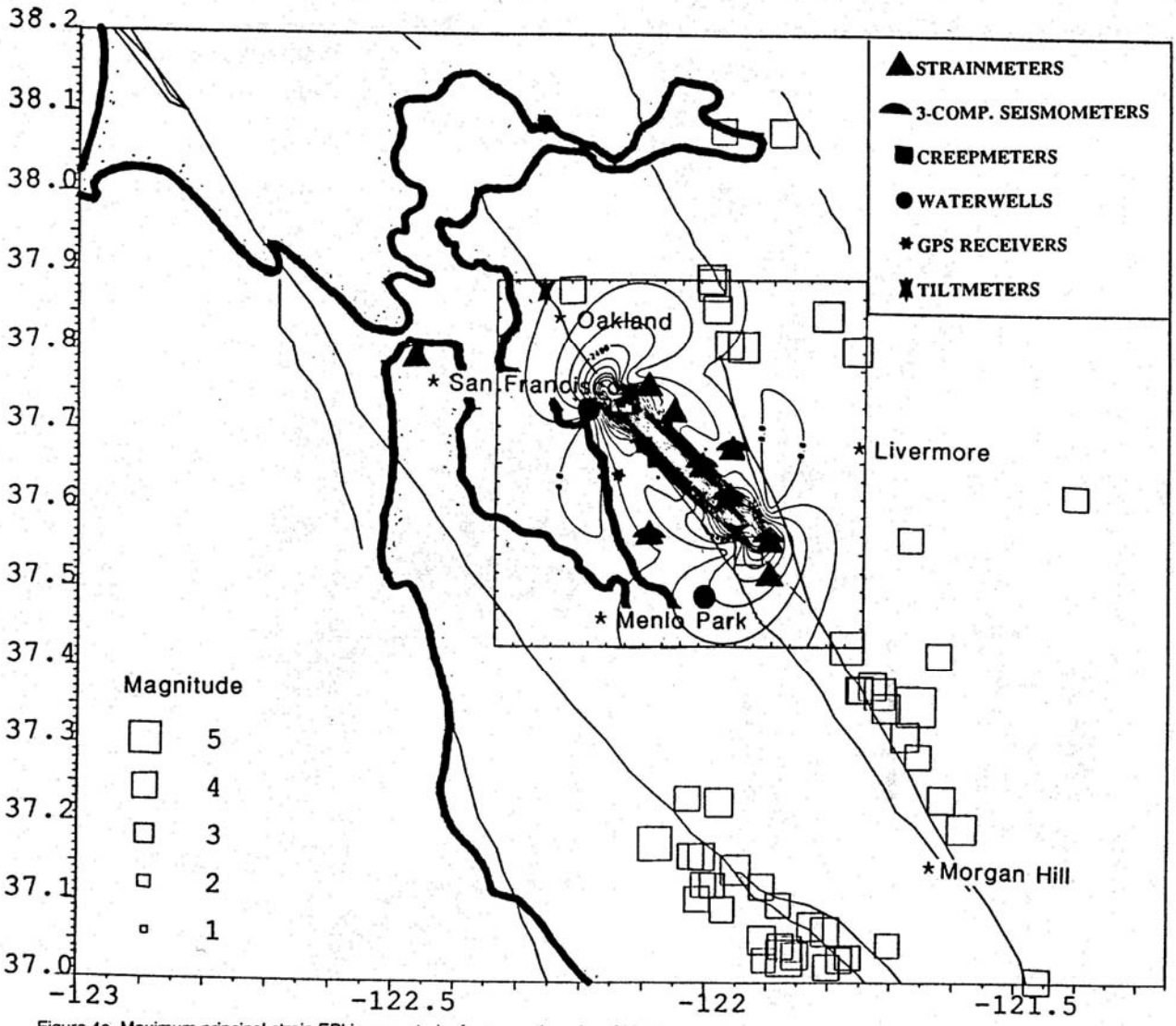

Figure 4a. Maximum principal strain EPI in nanostrain, for an earthquake of M 6.0 using the parameters shown in Table 1. The contours run from 0.0 to 10000 nanostrain with a contour interval of 600 nanostrain.

Table 1- Source Parameters for Hayward Earthquake Models

Parameter	Magnitude 5	Magnitude 6	Magnitude 6.5
*Depth (krn)	2	1	1
Strike (W of N)	45	45	45
Dip (N down)	90	90	90
Length (km)	7	20	30
Width (km)	3	IO	8
Slip (m)	0.05	0.16	I.00
+Moment	0.03	I.0	7.0

* Midpoint of top edge.

+ These moments have units of 10^{25}dyne-cm.

EXPECTED STRAIN AND DISPLACEMENT SIGNALS DURING EARTHQUAKES

To understand the form and amplitude of the expected strain and displacement signals, we have investigated models of likely earthquakes that could occur on the southern segment of the Hayward fault. This information also helps in designing the array of instruments for detection of these signals. We have modeled potentially damaging earthquakes with

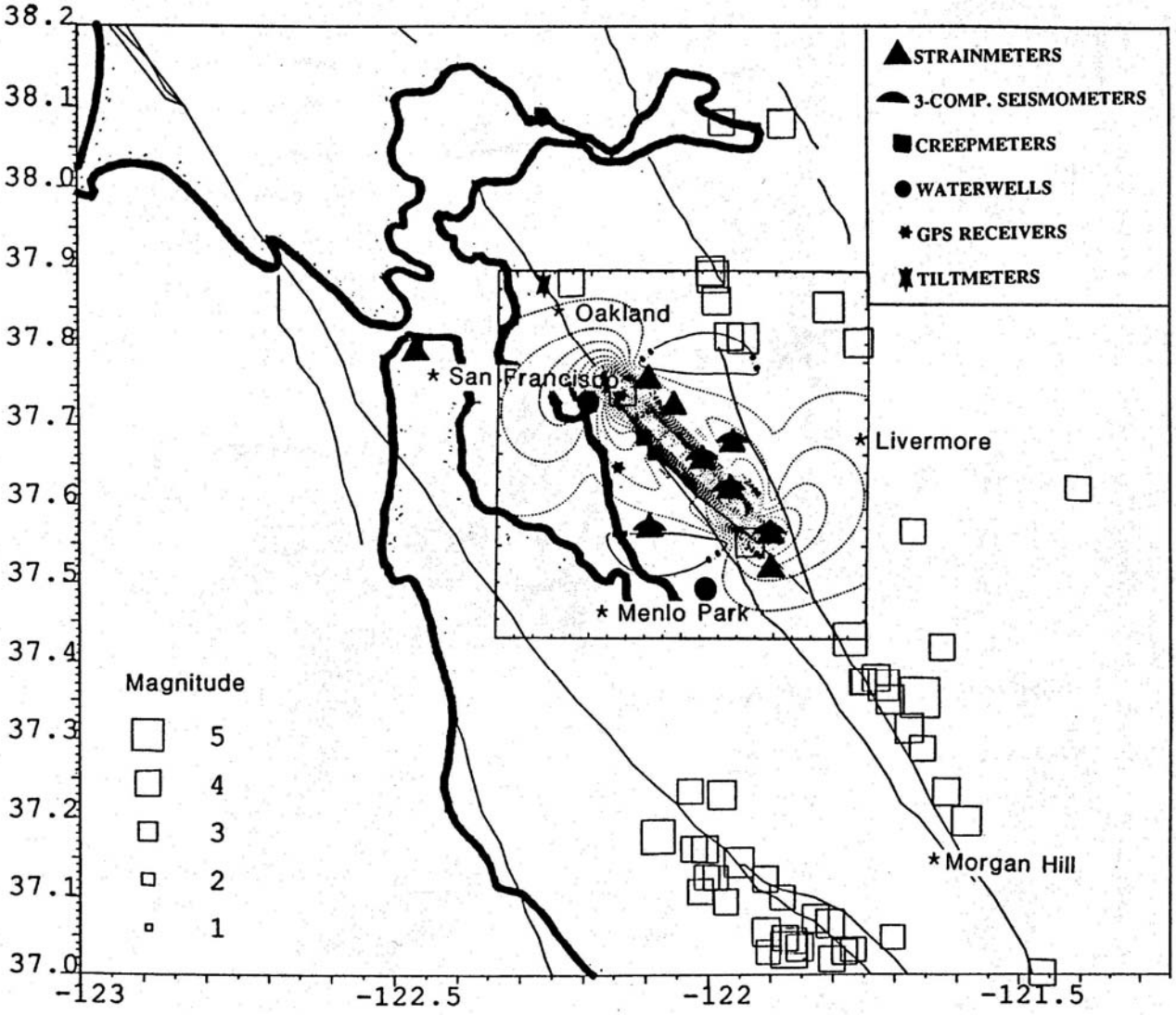

Figure 4b. Minimum principal strain EP2 in nanostrain, for an earthquake of M 6.0 using the parameters shown in Table 1. The contours run from -10000 to 0.0 nanostrain with a contour interval of 600 nanostrain.

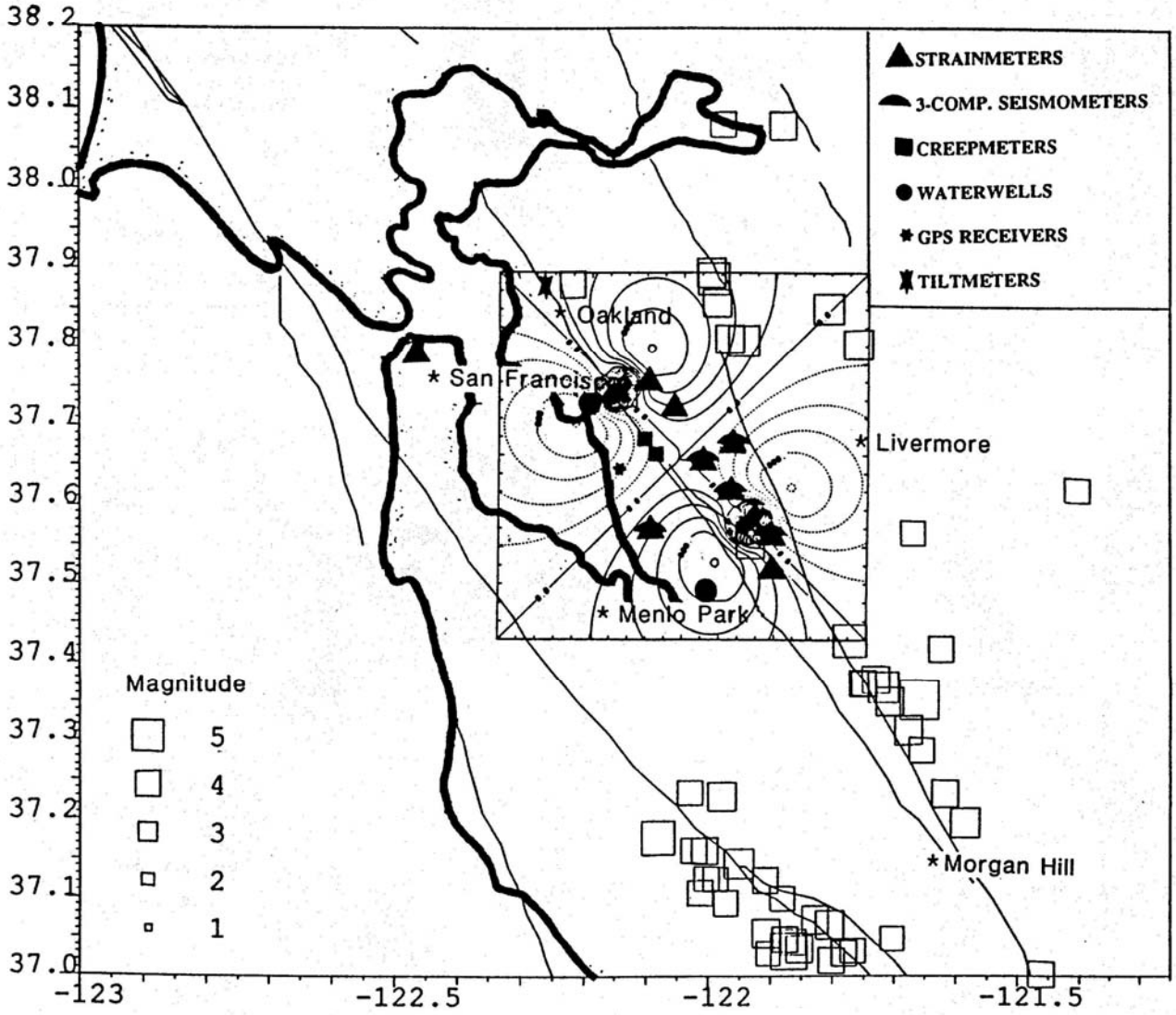

Figure 4c. Dilational strain in nanostrain, for an earthquake of M 6.0 using the parameters shown in Table 1. The contours run from -4000 to 4000 nanostrain with a contour interval of 200 nanostrain.

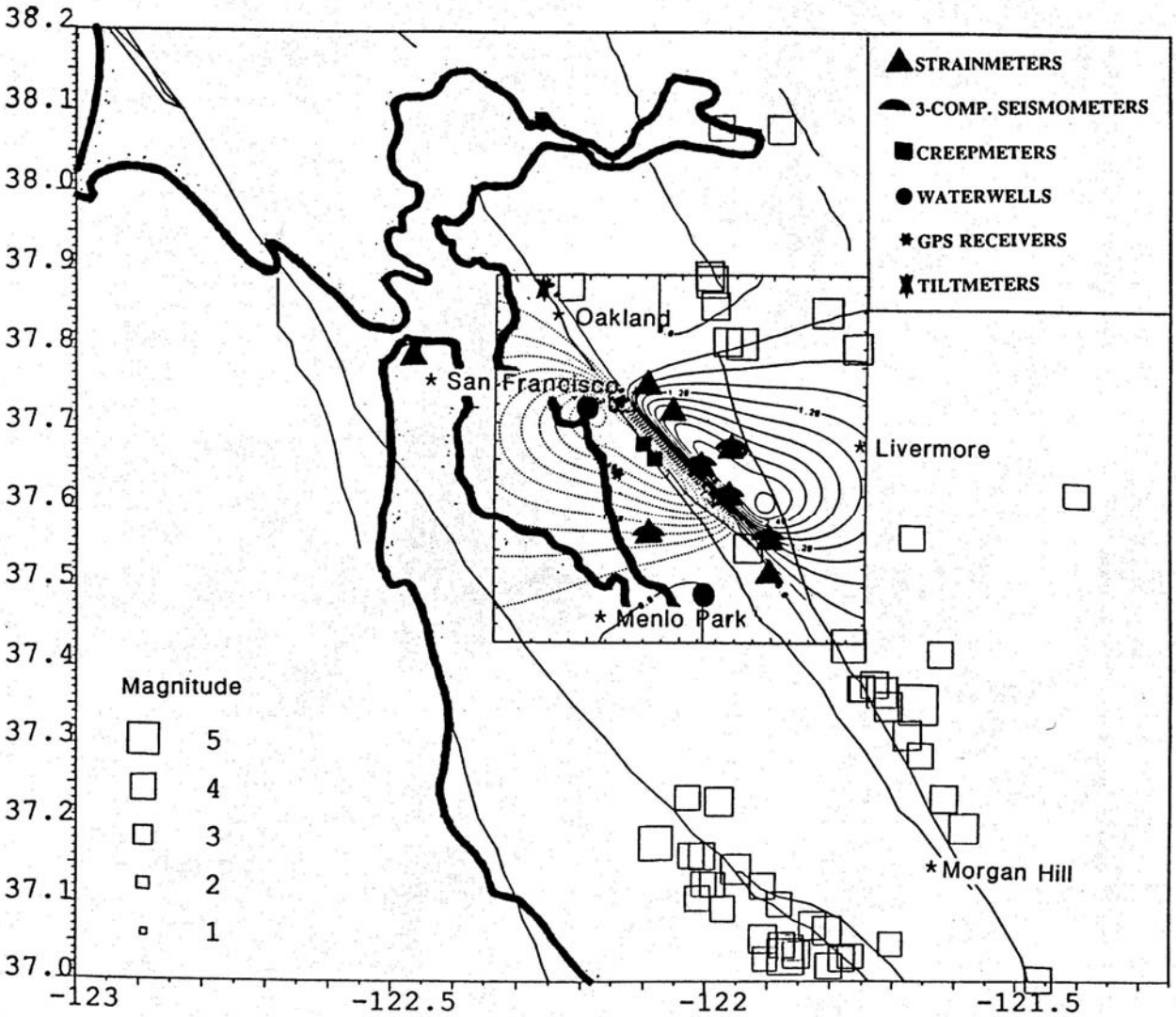

Figure 4d. Horizontal East-West surface displacements (in centimeters) for an earthquake of M 6.0 using the parameters shown in Table 1. Positive numbers represent displacements to the east. Contours run from -3.0 cm to 3.0 cm with a 3.0 mm contour interval.

magnitudes 5, 6, and 6.5 that could occur in this segment. The events are modeled as uniform slip on a simple rectangular fault patch using Okada's (1985) formulation for the surface deformations due to a dislocation embedded in an elastic half space. The particular parameters used for these models are shown in Table 1.

Figures 4a through 4e shows the maximum principle strain release (EPl, EP2), dilational strain release, North/South and East/West displacements expected in the Bay Area for an earthquake with M 6.0. For this earthquake L is 20 km, the width, W, of the rupture is 10 km with upper edge at a depth of 1 km and the amount of slip is 16 cm. The moment associated with this event is 10^{25} dyne-cm.

Models for earthquakes with magnitudes 5 and 4 have moments that are 33, and 1000 times smaller, respectively, than that for the magnitude 6.0 earthquake. A magnitude 6.5 is 7 times larger than the magnitude 6.0. While all of these events will be clearly recorded on all instruments in the strainmeter array only the largest (M 6 and M 6.5) will be detected in the GPS displacement measurements.

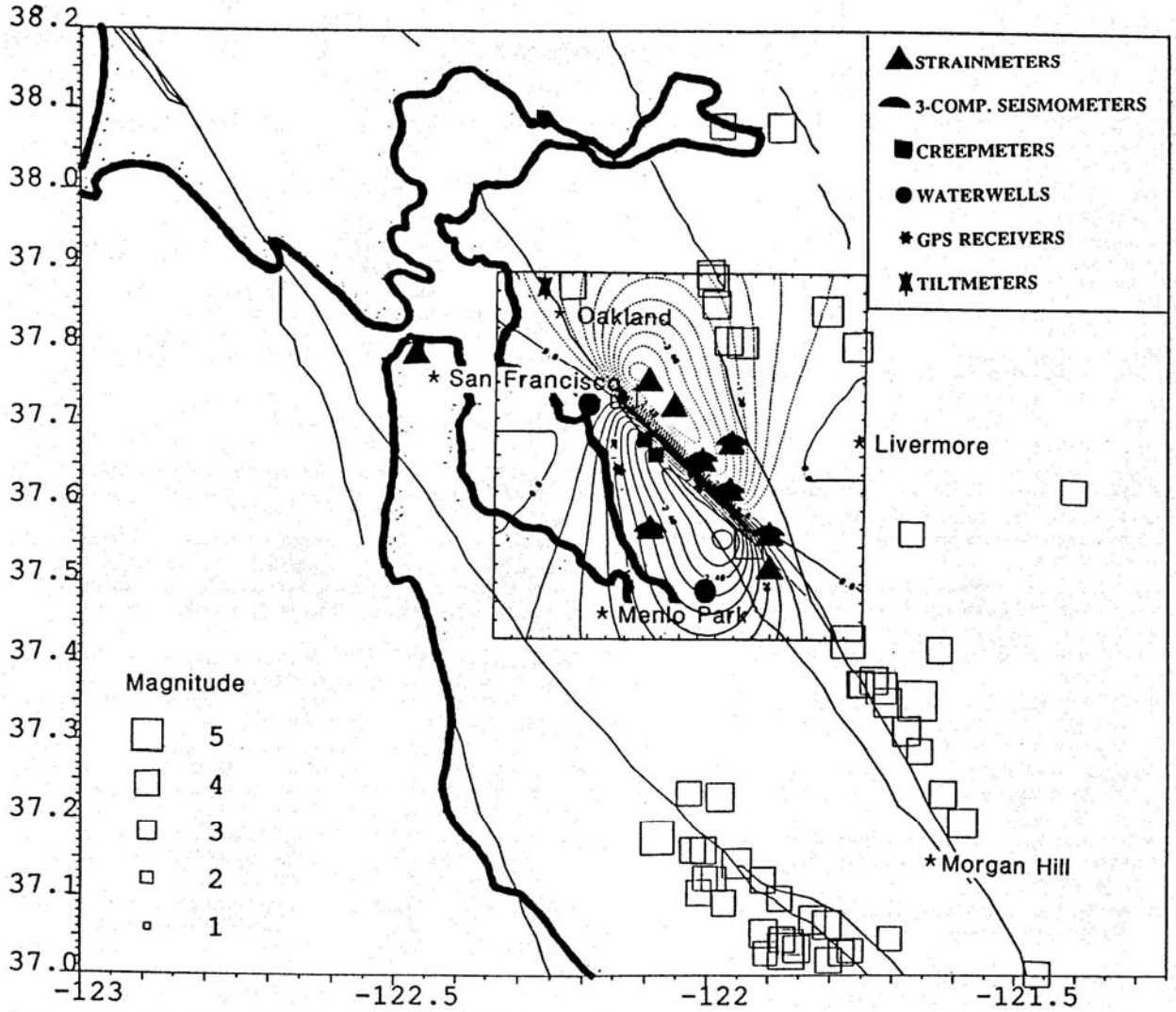

Figure 4e. Horizontal North-South surface displacements (in centimeters) for an earthquake of M 6.0 using the parameters shown in Table 1. Positive numbers represent displacements to the north. Contours run from -3.0 cm to 3.0 cm with a 3.0 mm contour interval.

CONCLUSIONS

[1] A prototype earthquake monitoring/prediction experiment is being installed along the southern segment of the Hayward fault to detect strain, ground displacement and ground velocity before and during any damaging earthquakes in this region..

[2] The experiment has been optimized to detect strains and displacements for earthquakes of about M 6 and greater and to search for the initiation of fault failure leading to these events.

[3] The maximum displacements and strains expected within 5 km of the Hayward fault will exceed 20 cm and 50 microstrain (50 ppm), respectively, for these earthquakes.

[4] Ample sensitivity exists with the borehole strainmeters to detect precursive strain at levels below 5 parts per billion (ie 10,000 times smaller than the strain occurring with these earthquakes). Observations along other active sections of the San Andreas fault (Johnston and others, 1987) indicate that strain associated with small earthquakes and aseismic fault slip will be observed with these instruments and may indicate the initiation of larger scale fault failure.

REFERENCES

Aki, K., 1987, Magnitude-frequency relation for small earthquakes: A clue to the origin of f_{max} of large earthquakes: Journal Geophysical Research, v. 92, p.1349-1355.

Andrews, D.J., 1976. Rupture velocity of plain-strain shear cracks. Journal Geophysical Research, v. 81, p. 5679-5687.

Borcherdt, R.D., Fletcher, J.B., Jensen, E.G., Maxwell, G.L., VanSchaack, J.R., Warrick, R.E., Cranswick, E., Johnston, M.J. S., McClearn, R., 1985, A General Earth Observation System (GEOS): Bulletin of the Seismological Society of America., v. 75, p.1783-1826.

Brune, J.N., 1979, Implications of earthquake triggering and rupture propagation for earthquake prediction based on premonitory phenomena: Journal of Geophysical Research, v. 84, p. 2195-2198.

Byerlee, J., 1990, Friction, overpressure, and fault normal compression: Geophysical Research Letters, v. 17, p. 2109-2112.

Das, S., and Scholz, C.H., 1981, Theory of time-dependent rupture in the earth: Journal of Geophysical Research, v. 86, p. 6039-6051.

Dieterich, J.H., 1979, Modeling of rock friction 1. Experimental results and constitutive equations: Journal of Geophysical Research, v. 84, p. 2161-2168.

Freund, L.B., 1979, The mechanics of dynamic shear crack propagation: Journal of Geophysical Research, v. 84, p. 2199-2209.

Gladwin, M.T., 1984, High precision multi-component borehole deformation monitoring: Review, Scientific Instruments, v. 55, p. 2011-2016.

Johnston, M.J.S., Borcherdt, R.D., Gladwin, M.T., Glassmoyer, G., and Linde, A.T., 1987, Fault failure with moderate earthquakes: Tectonophysics, v. 144, p. 189-206.

Kanamori, H., and Cipar, J.J., 1974, Focal processes of the great Chilean earthquake, May 22, 1966: Physics Earth Planetary Interiors, v. 9, p. 128-136.

Kostrov, B.V., 1966, Unsteady propagation of longitudinal shear cracks: Journal of Applied Mathematical Mechanics, v. 30, p. 1241-1248.

Linde, A.T., Suyehiro, K., Miura, S., Sacks, I.S., and Takagi, A., 1988, Episodic aseismic earthquake precursors: Nature, v. 334, p. 513-515.

Mogi, K., 1981a, Earthquake prediction program in Japan, *in* Simpson, D.W., and Richards, P.G., eds., Earthquake prediction: An international review: American Geophysical Union Monograph, p. 635-666.

Mogi, K., 1981b, Earthquake prediction and rock mechanics: Journal of the Society of Material Science, Japan, v. 30, p. 105-118.

Mogi, K., Yoshikawa, S., and Kogita, S., 1982, Changes preceding the sudden slip of artificial fault planes (2) - precursory deformation [abs.]: Seismological Society, Japan, v. 1, p.128.

Mogi, K., 1985, Earthquake prediction: Academic Press, New York, 355 p.

Okada, Y., 1985, Surface deformation due to shear and tensile faults in a half-space: Bulletin of the Seismological Society of America, v. 75, p. 1135-1154.

Rice, J.R., 1983. Constitutive relations for fault slip and earthquake instabilities: Pure Applied Geophysics, v. 121, p. 443-475.

Rice, J.R. 1992. Fault stress states, pore pressure distributions, and the weakness of the San Andreas fault, *in* Evans, Brian, and Wong, Teng-Fong, eds, Fault mechanics and transport properties of rock: A festchrift in honor of W.F. Brace: Academic Press, New York.

Rice, J.R., and Rudnicki, J.W., 1979. Earthquake precursory effects due to pore fluid stabilization of a weakening fault zone: Journal of Geophysical Research, v. 84, p. 2177-2193.

Richards, P.G., 1976. Dynamic motions near an earthquake fault: A three-dimensional solution: Bulletin of the Seismological Society of America, v. 65, p. 93-112.

Rikitake, T., 1976, Earthquake prediction, Elsevier, New York, p 357.

Rundle, J.B., Kanamori, H., and McNally, K.C., 1984, An inhomogeneous fault model for gaps, asperities, barriers, and seismologicalic migration: Journal of Geophysical Research, v. 89, p. 10,219-10,231.

Sacks, I.S., Suyehiro, S., Evertson, D.W., and Yamagishi, Y., 1971, Sacks-Evertson strainmeter, its installation in Japan and some preliminary results concerning strain steps: Papers on Meteorology and Geophysics, v. 22, p. 195-207.

Sadovsky, M.A., Nersesov, I.L., Nigmatullaev, S.K., Latynina, L.A., Lukk, A.A., Semenov, A.N., Simbireva, I.G., and Ulomov, V.I., 1972, The processes preceding strong earthquakes in some regions of Middle Asia: Tectonophysics, v.14, p. 295-307.

Schulz, S.S., and Burford, R.O., 1979, Catalog of creep measurements in central California for 1976 and 1977: U.S. Geological Survey Open-File Report 79-1609, 375 p.

Silverman, S., Mortensen, C., and Johnston, M.J.S.,1989, A satellite-based digital data system for low-frequency geophysical data: Bulletin of the Seismological Society of America, v. 79, p.189-198.

Stuart, W.D., 1979. Strain softening prior to two dimensional strike-slip earthquakes: Journal of Geophysical Research, v. 84, p. 1063-1070.

Stuart, W.D., and Mavko, G., 1979, Earthquake instability on a strike-slip fault: Journal of Geophysical Research, v. 84, p. 2153-2160.

Wyatt, F., Beckstrom K., and Berger, J., 1982, The optical anchor - A geophysical strainmeter: Bulletin of the Seismological Society of America, v. 72, p. 1707-1715.

ACKNOWLEDGEMENTS

We thank Glenn Borchardt and an anonymous reviewer for reviewing this manuscript. In particular, we thank the East Bay Regional Park District, Mr. and Mrs. D. Ham, Gelderman Enterprises, and the Delucci Management Group for permission to use these sites for this purpose.